Molecular mechanisms underlying cellular effects of human MEK1 mutations

Robert A. Marmion[a,†], Liu Yang[a,†], Yogesh Goyal[a,b,c,‡], Granton A. Jindal[a,b,d,‡], Joshua L. Wetzel[a,e], Mona Singh[a,e], Trudi Schüpbach[f], and Stanislav Y. Shvartsman[a,b,f,g,*]

[a]Lewis-Sigler Institute for Integrative Genomics, [b]Department of Chemical and Biological Engineering, and [f]Department of Molecular Biology, Princeton University, Princeton, NJ 08544; [g]Flatiron Institute, Simons Foundation, New York, NY 10010; [e]Department of Computer Science, Princeton University, Princeton, NJ 08540; [c]Department of Bioengineering, University of Pennsylvania, Philadelphia, PA 19104; [d]Department of Medicine, University of California San Diego, La Jolla, CA 92093

ABSTRACT **Terminal regions of *Drosophila* embryos are patterned by signaling through ERK, which is genetically deregulated in multiple human diseases. Quantitative studies of terminal patterning have been recently used to investigate gain-of-function variants of human MEK1, encoding the MEK kinase that directly activates ERK by dual phosphorylation. Unexpectedly, several mutations reduced ERK activation by extracellular signals, possibly through a negative feedback triggered by signal-independent activity of the mutant variants. Here we present experimental evidence supporting this model. Using a MEK variant that combines a mutation within the negative regulatory region with alanine substitutions in the activation loop, we prove that pathogenic variants indeed acquire signal-independent kinase activity. We also demonstrate that signal-dependent activation of these variants is independent of kinase suppressor of Ras, a conserved adaptor that is indispensable for activation of normal MEK. Finally, we show that attenuation of ERK activation by extracellular signals stems from transcriptional induction of Mkp3, a dual specificity phosphatase that deactivates ERK by dephosphorylation. These findings in the *Drosophila* embryo highlight its power for investigating diverse effects of human disease mutations.**

Monitoring Editor
Richard Fehon
University of Chicago

Received: Oct 5, 2020
Revised: Jan 7, 2021
Accepted: Jan 15, 2021

INTRODUCTION

Somatic mutations in genes encoding components of the RAS pathway have been recognized as drivers of tumorigenesis since the 1990s (Hanahan and Weinberg, 2000; Avruch, 2007; Roberts and Der, 2007; Hanahan and Weinberg, 2011; Poulikakos and Solit, 2011; Chapman *et al.*, 2014). More recently, germline mutations in the same genes have been associated with developmental diseases, collectively known as RASopathies (Rauen, 2013; Edwards and Gelb, 2016). These mutations, estimated to affect ~1/1000 human births, produce a broad spectrum of phenotypes, including heart defects, stunted growth, and neurocognitive impairments (Tartaglia and Gelb, 2010; Maher *et al.*, 2016, 2018b). Hundreds of such mutations have already been identified and many more are likely to be discovered by personalized sequencing projects. What is sorely lacking, however, is a rigorous strategy for investigating the functional consequences of these mutations in vivo. To address this challenge, we have recently started to use quantitative experiments

This article was published online ahead of print in MBoC in Press (http://www.molbiolcell.org/cgi/doi/10.1091/mbc.E20-10-0625) on January 21, 2021.

†Authors contributed equally.

‡Current address.

Author contributions: conceptualization, R.A.M., L.Y., Y.G., G.A.J., T.S., and S.Y.S.; experimental design, R.A.M., L.Y., Y.G., G.A.J., and S.Y.S.; experimental implementation, R.A.M. and L.Y.; RNA-seq analysis and visualization, J.W. and R.A.M.; writing—original draft, R.A.M., L.Y., and S.Y.S.; writing—review and editing, R.A.M., L.Y., Y.G., G.A.J., T.S., and S.Y.S.; supervision, S.Y.S. and M.S.; funding acquisition, S.Y.S.

Declaration of interests: the authors declare no competing interests.

*Address correspondence to: Stanislav Y. Shvartsman (stas@princeton.edu).

Abbreviations used: CFC, cardiofaciocutaneous syndrome; KSR, kinase suppressor of Ras; NRR, negative regulatory region; RNAi, RNA interference; RNA-seq, RNA sequencing; RTK, receptor tyrosine kinase.

in *Drosophila*, capitalizing on the reproducible nature of endogenous signaling events and on the large suite of techniques for targeted genetic perturbations at essentially all levels of the RAS pathway (Ashton-Beaucage and Therrien, 2017).

The present study is motivated by a feedback model that has emerged from our work on mutations affecting *MEK1* kinase (Goyal *et al.*, 2017a), a core component of pathway (Bromberg-White *et al.*, 2012; Futran *et al.*, 2013). Kinase activity of MEK requires its phosphorylation by RAF, an upstream kinase of the RAS cascade (Futran *et al.*, 2013). We discovered that although pathogenic variants are clearly activating at the molecular level, they can cause both ectopic pathway activation and reduction of its sensitivity to extracellular signals (Jindal *et al.*, 2015; Goyal *et al.*, 2017a, b). Both effects could be explained using a mathematical model whereby the RAF-independent activity of a mutant kinase triggers the expression of inhibitors that desensitize the pathway to future activation by extracellular cues. Here we provide direct proof of this model by identifying the molecular nature of the negative feedback. Furthermore, we extend our mechanistic analysis of activating mutations and show that they make MEK1 independent of KSR, an adaptor protein which is essential for ligand-dependent signal transduction under normal conditions (Patel and Shvartsman, 2018).

Our approach to quantitative studies of disease mutations relies on imaging pathway activation in the early *Drosophila* embryo, a time when *all* intracellular pathway components are uniformly expressed but remain inactive until signal transduction is initiated by locally secreted extracellular ligands of the cell surface receptor tyrosine kinases (RTKs) (Figure 1A). The first of these RTKs is Torso, which is provided with the active form of ligand (Trunk) at the poles of the embryo (Goyal *et al.*, 2018). Torso signaling is responsible for the RAS-dependent induction of genes involved in the formation of the nonsegmented terminal structures of the future larva. RAS signaling induced by Torso can be visualized in several ways, including immunohistochemistry using antibodies recognizing the dually phosphorylated form of ERK (dpERK), the terminal kinase of the RAS pathway, and a direct substrate of active MEK (Gabay *et al.*, 1997). We established a robust approach for pairwise comparison of ERK activation between normal (wild type [WT]) and genetically perturbed embryos (Coppey *et al.*, 2008). In particular, one can study the effect of targeted expression of disease variants of MEK.

We used the Gal4-UAS system to overexpress MEK variants on top of normal levels of WT MEK (Duffy, 2002). We used GFP-labeled WT embryos as internal control for all experimental quantification Additionally, we have previously demonstrated that mutant MEK has no difference in protein stability or localization (Goyal *et al.*, 2017a). Importantly, we additionally showed that increased levels of WT MEK do not affect the pattern of ERK activation, which means that MEK is not a limiting pathway component and provides a reference point for quantifying the effects caused by targeted expression of disease variants (Goyal *et al.*, 2017a). We use this feature of RAS signaling in the early embryo to experimentally test the main assumptions of our model: ligand-independent MEK activity and transcriptional induction of a negative regulator. Most of our experiments use the MEK^{F53S} variant, which was identified in individuals with cardiofaciocutaneous syndrome (CFC), a form of RASopathy that is characterized by mild craniofacial dysmorphia and pulmonary valve stenosis (Figure 1, B and C) (Rauen, 1993). Since the MEK^{F53S} substitution impacts the negative regulatory region (NRR) which keeps MEK inactive in the absence of phosphorylation by RAF, MEK^{F53S} can be partially active even in cells not exposed to RTK signaling (Fischmann *et al.*, 2009). Here we provide direct proof of RAF-independent activity in vivo and show that it causes the expression of an ERK phosphatase. We used genetic experiments to show that it is indeed the critical component of the feedback loop. We also show that MEK^{F53S} is more sensitive to activation by ligands and suggest that this is a common property of disease variants.

RESULTS

RAF-independent kinase activity

In contrast to what is observed with WT MEK, overexpression of MEK^{F53S} and other disease variants leads to significant changes in the spatial pattern of active ERK: it is significantly elevated in the middle of the embryo and strongly down-regulated at the poles (Goyal *et al.*, 2017a). Ectopic activation in the region maximally removed from the poles, where the diffusible ligand of Torso is produced, can be explained in two, nonmutually exclusive ways. Mutant MEKs can be enzymatically active even in the absence of ligand-dependent phosphorylation by RAF, which can be caused by disrupted intramolecular interactions with the NRR of MEK (Fischmann *et al.*, 2009; Jindal *et al.*, 2017a). Mutant MEKs can also be more sensitive to extracellular ligands, which can induce RAF-dependent phosphorylation and kinase activation even at residual levels of Torso ligand that are insufficient for causing activation of WT MEK (Yeung *et al.*, 2020).

The differential contributions of two effects can be probed using a protein that combines the MEK^{F53S} substitution with two alanine substitutions of the two serines that are phosphorylated by RAF and are essential for activation of WT MEK (Mansour *et al.*, 1996). If ectopic activation in the middle of the embryo is caused solely by RAF-independent activity, it should be indistinguishable from the effect caused by overexpression of the unphosphorylatable MEK^{F53S} variant (MEK$^{F53S\ SSAA}$) (Figure 1D). To test this prediction, we generated transgenic flies in which the UAS construct controlling such a variant is inserted in the same region of the genome as the UAS-MEK constructs used in our earlier studies. We found that the midembryo ERK activation by the double mutant was significantly increased relative to the WT ($p = 0.000131$), just like the variant with an intact activation loop ($p = 0.000471$) (Figure 1, E–G; Supplemental Figure S1). We also detected significant down-regulation of ERK activation at the poles, since strongly overexpressed mutant protein competes with endogenous MEK and interferes with its phosphorylation and activation by RAF. Caution should be utilized when comparing the poles of these two mutants, since this dominant-negative effect caused by the SSAA mutation is different from the induced negative feedback that we have previously described with GOF mutations (Goyal *et al.*, 2017a). We will address this in the final section of the paper. What is more important for the current work is the effect in the middle of the embryo, which unambiguously establishes small but measurable catalytic activity of unphosphorylated MEK^{F53S} and is consistent with previous kinetic data from studies with purified MEK and ERK proteins (Jindal *et al.*, 2017a; Yeung *et al.*, 2020).

Increased sensitivity to activation by RAF

Several MEK disease variants, including MEK^{F53S}, display an increased rate of phosphorylation by RAF in vitro, suggesting that they are more sensitive to activation by extracellular signals in vivo (Yeung *et al.*, 2020). However, in vitro studies that led to this conclusion relied on a binary system containing MEK1 and preactivated RAF, whereas MEK activation in vivo requires kinase suppressor of Ras (KSR), a protein scaffold essential for the RTK-dependent ERK signaling (Therrien *et al.*, 1995; Udell *et al.*, 2011). KSR forms heterotrimeric complexes with both MEK and RAF, which is critical both for the allosteric activation of RAF and for the RAF-dependent activation of WT MEK (Brennan *et al.*, 2011; Dhawan *et al.*, 2016;

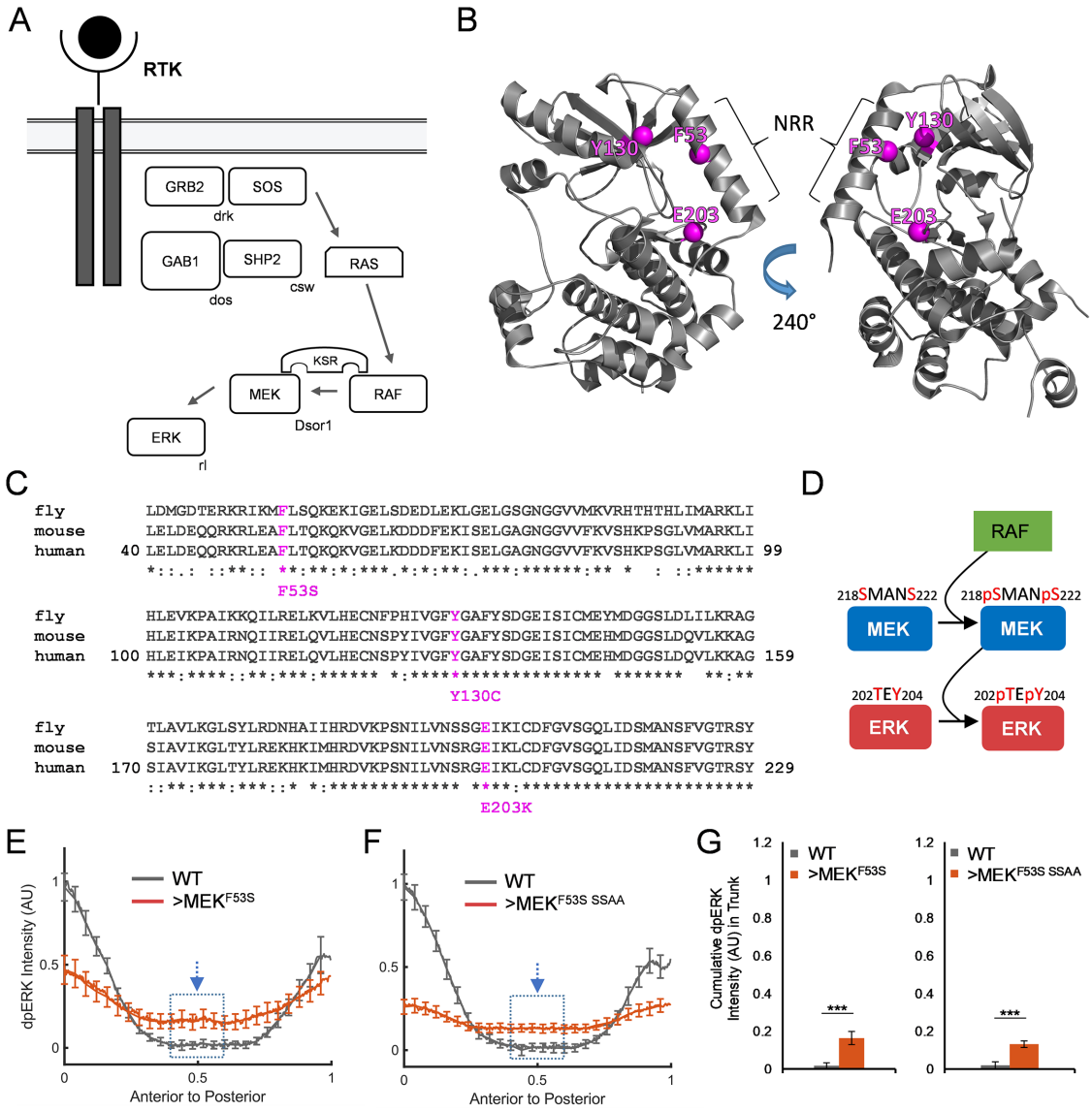

FIGURE 1: Testing ligand-independent signaling. (A) Simplified schematic of the *Drosophila* RAS signaling pathway, showing the key components. *Drosophila* gene names are listed under their conserved homologue. (B) Structural model of MEK1 from two perspectives. Mutated positions utilized throughout the paper are colored in magenta. The NRR is indicated by a bracket. (C) Multiple alignment showing conservation domain residues. Highlighted (in magenta) are three mutations used in this study: two from RASopathies (F53S and Y130C) and one from cancer (E203K). (D) In the presence of signaling through RAF, MEK is phosphorylated at serines at positions 218 and 222. Dually phosphorylated MEK then phosphorylates ERK at a threonine-tyrosine pair at positions 202 and 204, respectively. (E, F) Pairwise comparisons of the spatial dpERK profiles in nuclear cycle 14 embryos for WT (gray) and mutant (red) embryos. (E) WT ($n = 12$) and MTD>MEK^{F53S} ($n = 13$) (Goyal *et al.*, 2017a). (F) WT ($n = 13$) and MTD>MEK$^{F53S\ S218A\ S222A}$ (referred to as MTD>MEK$^{F53S\ SSAA}$) ($n = 26$). Error bars denote standard error of the mean. (G) Bar graphs of the in vivo constitutive activity in the middle of the embryo (blue dashed box in E and F) of MTD>MEK^{F53S} and MTD>MEK$^{F53S\ SSAA}$. The WT controls are in gray, while the mutants are in red. *P* values are obtained by Student's *t* test (two-sided, homoscedastic): ***$P < 0.001$.

Lavoie *et al.*, 2018). Given the critical role of KSR in the activation of WT MEK, we examined the effects on disease variants.

Consistent with its essential role in the RTK-dependent signaling, we found that ERK activation by Torso is abolished when *ksr* expression is depleted by RNA interference (RNAi) (Figure 2, A and D). Remarkably, this effect could be significantly rescued by expressing the MEK^{F53S} variant (Figure 2, B and E). Importantly, expression of the WT MEK could not rescue the effect of *ksr* knockdown (Figure 2, C and F). The rescuing effect is also seen by examining the transcriptional effects of ERK activation by Torso (Casanova and Struhl, 1989; Smits and Shvartsman, 2020). Specifically, ERK signaling at the termini induces the expression of zygotic genes needed for the formation of the terminal structures of the future larva. One of these genes, *tailless* (*tll*), is expressed in both anterior and posterior domains (Strecker *et al.*, 1986). The anterior domain of *tll* reflects the joint action of several patterning cues, but the posterior domain depends on Torso alone and serves as a sensitive readout of pathway activation (Figure 2G) (Kim *et al.*, 2013). Consistent with the

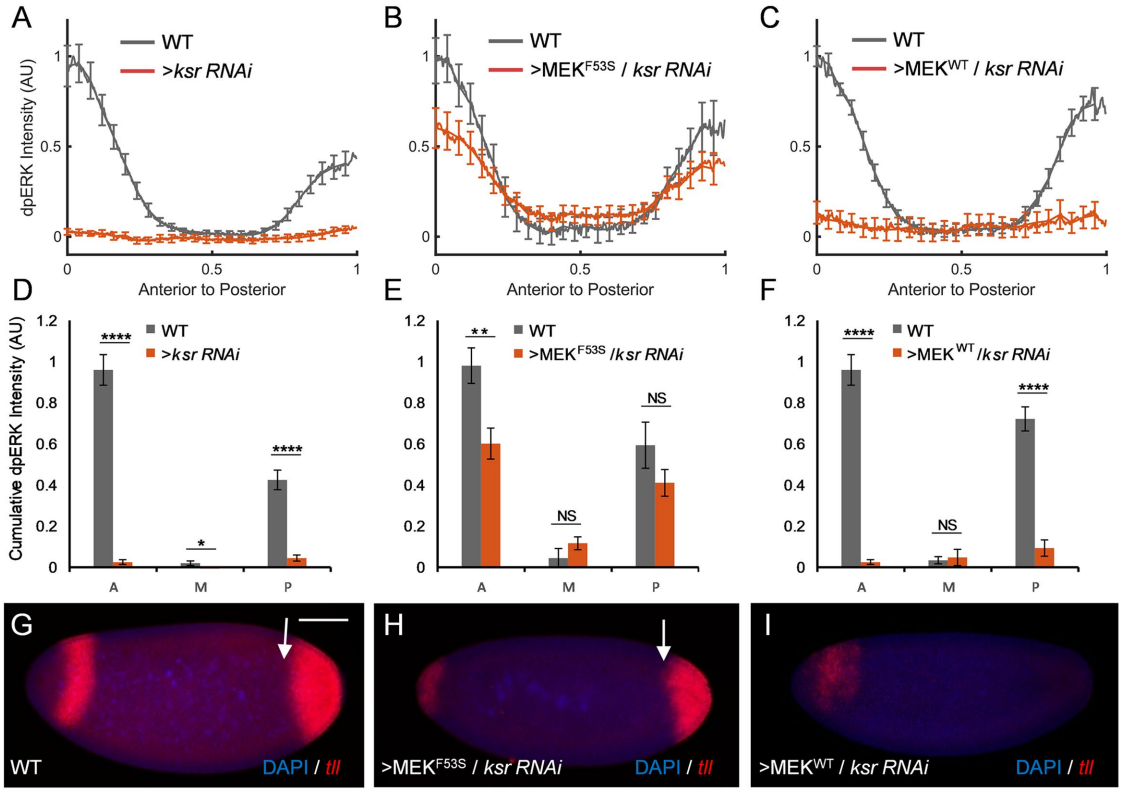

FIGURE 2: Increased sensitivity to extracellular signals. (A–C) Pairwise comparisons of the spatial dpERK profiles in nuclear cycle 14 embryos for WT (gray) and mutant (red) embryos. (A) WT ($n = 11$) and MTD> *ksr* RNAi ($n = 11$). (B) WT ($n = 10$) and MTD>MEK^{F53S} + *ksr* RNAi ($n = 23$). Error bars denote standard error of the mean. (C) WT ($n = 10$) and MTD>MEK^{WT} + *ksr* RNAi ($n = 24$). (D–F) Comparative analysis of dpERK levels in the anterior (A), middle (M), and posterior (P). regions of the embryo. The analysis performed corresponds to the same embryo data used to generate the spatial plots in A–C. *P* values were obtained by Student's *t* test (two-sided, homoscedastic): ****$P < 0.0001$, **$P < 0.01$, *$P < 0.05$, NS: $P > 0.05$. Error bars denote standard error of the mean. (G–I) Fluorescence in situ hybridization for *tailless* (*tll*) in nuclear cycle 14 embryos. Arrows denote the boundaries of *tll* expression. (G) WT. (H) MTD>MEK^{F53S} + *ksr* RNAi, *tll* expression was rescued in the posterior. (I) MTD>MEK^{WT} + *ksr* RNAi, *tll* expression was eliminated in the posterior of the embryo. Scale bar, 75 μm.

effects of *ksr* depletion on Torso-dependent ERK activation, we found that complete loss of posterior *tll* expression in the *ksr* knockdown embryos is substantially rescued by the concurrent overexpression of MEK^{F53S} but not WT MEK (Figure 2, H and I). Thus, in contrast to WT MEK, the disease MEK variant can be activated by RAF independently of KSR. The middle of the embryo, which normally is not subject to ERK signaling, provides a readout of the quantity of constitutive activity by mutant MEK. The slight increase that we see in the middle of the MEK^{F53S} mutant is not enough to explain the substantial increase of signaling that we measure in the termini, which strongly suggests that rescue is indeed ligand dependent.

This conclusion is further supported by analyzing the morphogenetic effects of terminal signaling, such as the formation of the larval filzkörper, tubular structures needed for respiration (Figure 3, A and A′, green arrowhead) (Jurgens *et al.*, 1984; Dalton *et al.*, 1989). Consistent with previous studies, embryos with RNAi-depleted *ksr* or *raf* fail to form filzkörper (Figure 3, B–C′, B′ and C′, gray arrowhead). However, filzkörper are restored in a significant fraction of embryos where *ksr* depletion is combined with expression of MEK^{F53S} (Figure 3, D and D′). Importantly, overexpression of WT MEK does not rescue filzkörper (Figure 3, E and E′). Even though the rescuing capacity of the MEK^{F53S} variant does not require KSR, we found that it still depends on RAF and is lost in embryos where expression of MEK^{F53S} was combined with the knockdown *raf* (Figure 3, F and F′). This means that the rescuing effect of MEK^{F53S} is strictly dependent on upstream signaling. Importantly, the KSR-independent rescuing ability was not limited to a single MEK variant and was also observed for the E203K and Y130C variants that were identified in human cancer and CFC syndrome, respectively (Figure 3, G and I) (Rodriguez-Viciana *et al.*, 2006; Bentivegna *et al.*, 2008).

Transcriptional induction of Mkp3 by constitutively active MEK

How can MEK variants that have signal-independent activity and are also more prone to activation by extracellular signals cause a strong reduction of ERK activation by Torso in the terminal regions of the embryo? We proposed that this paradoxical behavior is caused by a hypothetical inhibitor of ERK activation that is induced by constitutive activity of MEK variants and desensitizes the ERK cascade to activation by RTK ligands (Goyal *et al.*, 2018). Genetic studies in *Drosophila* and other model systems have identified several inhibitors, such as Sprouty, that are transcriptionally induced by ERK and can inhibit ERK activation at multiple points within the ERK cascade (Musacchio and Perrimon, 1996; Sawamoto *et al.*, 1996; Casci *et al.*, 1999; Neben *et al.*, 2019). Negative regulators may be expressed in a tissue-specific manner, rendering certain tissues particularly sensitive to increased RAS signaling as was suggested for germline mutations of HRAS in mice (Chen *et al.*, 2009). Functional

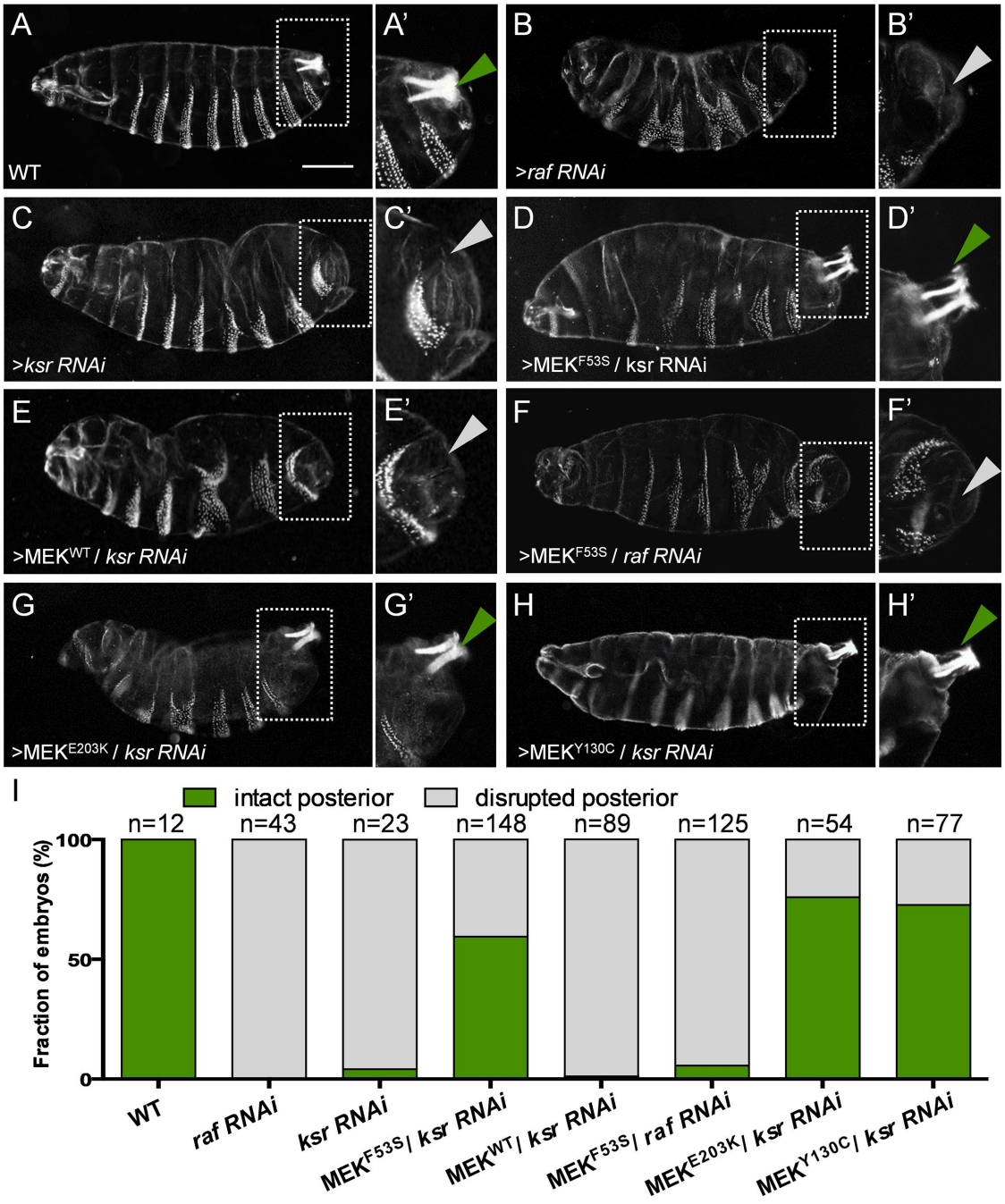

FIGURE 3: Rescue of posterior patterning in the absence of KSR. (A–H′) Cuticle phenotypes from indicated genotypes. Posterior regions are enlarged to show the presence or absence of filzkörper. Green arrowheads denote the presence of filzkörper and gray arrowheads denote the absence of the filzkörper. (A) WT. (B) MTD>*raf* RNAi. (C) MTD>*ksr* RNAi. (D) MTD>MEK^{F53S} + *ksr* RNAi. (E) MTD>MEK^{WT} + *ksr* RNAi. (F) MTD>MEK^{F53S} + *raf* RNAi. (G) MTD>MEK^{E203K} + *ksr* RNAi. (H) MTD>MEK^{Y130C} + *ksr* RNAi. Scale bar, 130 μm. All primes are all insets to zoom in on the filzkörper of the corresponding image. (I) Quantification of filzkörpers for indicated genotypes.

effects of these feedbacks on pathway activation and function in vivo are underexplored.

As an unbiased way of identifying the candidate regulators that could potentially explain the observed desensitization of the ERK cascade in our system, we used RNA sequencing (RNA-seq) to compare maternally deposited transcripts in embryos from mothers expressing either MEK^{F53S} or WT MEK (Figure 4A). We found that signal-independent constitutive activity of MEK^{F53S} leads to pronounced ERK activation in the nurse cells, which are connected to the oocyte by stable cytoplasmic bridges and supply the future oocyte with multiple cytoplasmic components, including all maternally deposited transcripts encoding the RAS pathway components (Supplemental Figure S2). This observation is crucial, since it highlights that previous stages of development contribute to subsequent developmental events. We hypothesized that ectopic ERK signaling changes the sensitivity to subsequent ERK signaling through transcriptional feedbacks in the maternal contribution in the unfertilized embryo. This is important, since we have not observed the negative feedback

in optogenetic stimulation of the ERK pathway, where pathway stimulation was limited to the early embryo (Johnson *et al.*, 2017).

Our analysis revealed significant changes in the expression of known transcriptional targets of ERK signaling, such as *pnt, aos*, and *mkp3*, demonstrating that maternal expression of constitutively active MEK indeed changes the composition of maternally deposited transcriptome. We focused on Mkp3, a dual specificity phosphatase that dephosphorylates dually phosphorylated ERK and is transcriptionally induced by the ERK pathway in developing and adult tissues (Figure 4B) (Keyse, 2008; Haagenson and Wu, 2010; Seternes *et al.*, 2019). We note that these signaling changes occur before the maternal-zygotic transition, which leaves no time for a patterned transcriptional response. The up-regulation of *Mkp3* that we measure in our RNA seq experiments must therefore be occurring already during oogenesis in the nurse cells and this RNA is then imported into the oocyte during oogenesis. Therefore, if the additional maternal *Mkp3* remains uniformly distributed in the early embryo as it is in WT (Gomez *et al.*, 2005), we expect a global effect on ERK signaling, both at the poles and the middle of the embryo. Indeed, that is what we see. Furthermore, if the MEK-induced induction of *Mkp3* is responsible for the reduction of ERK signaling at the poles (Figure 4, C, E, F, and I), knockdown of *mkp3* should restore normal levels of ERK signaling. We could directly test this prediction by using the same maternal driver to express both constitutively active MEK and RNAi targeting *Mkp3*. Remarkably, embryos from these mothers had near-normal levels of active ERK at the poles and even increased active ERK in the middle of the embryo, confirming a global effect of Mkp3 (Figure 4, D, E, G, and J). Importantly, maternal RNAi knockdown of *Mkp3* had no effect without constitutively active MEK (Figure 4, H and K). These results strongly support the model whereby the Mkp3-dependent feedback is activated by the constitutively active MEK and causes reduction of the ERK pathway activation by Torso (Goyal *et al.*, 2017a).

DISCUSSION

Understanding how coding mutations in human MEK1 affect ERK signaling in vivo is important both for clinical applications and for fundamental research. First, since multiple components of the ERK cascade, including MEK, are drug targets in oncology and other therapeutic areas, it is critical to determine how the effects of candidate drugs are impacted by mutations (Ohren *et al.*, 2004; Caunt *et al.*, 2015). Second, it is important to investigate how disease mutations perturb the elaborate mechanisms that have been elucidated by decades of work on MEK regulation and function. In theory, one could start from structural information for WT MEK and try to predict the effects of mutations using molecular dynamics simulations (Nikolaev *et al.*, 2011; Ordan *et al.*, 2018). In practice, however, computational tools are yet to access the timescales relevant for protein complexes involved in MEK regulation and function. Another approach is based on reconstitution of isolated processes in vitro, such as MEK phosphorylation by RAF (Jindal *et al.*, 2017a; Yeung *et al.*, 2020). While this approach is commonly used as a useful step in functional characterization of disease mutations, extrapolating the results of in vitro studies to signaling in crowded and compartmentalized intracellular systems is nontrivial.

Given the challenges faced by computational and reconstitution strategies to mechanistic studies of disease mutations, it appears more promising to analyze how they influence ERK signaling in cells and tissues. The terminal patterning system is well suited for this purpose because it is readily accessible to quantitative analysis of ERK signaling and its transcriptional and morphogenetic defects and can be genetically perturbed at multiple levels of the ERK cascade (Goyal *et al.*, 2018). We used these advantages to investigate the signaling properties of MEK variants that have been predicted to cause signal-independent activity of MEK and/or accelerate signal-dependent MEK activation (Fischmann *et al.*, 2009; Jindal *et al.*, 2017a; Yeung *et al.*, 2020). Using a variant that combines alanine substitutions with the activation loop with mutations within the negative regulation of MEK, we established that disease variants indeed have enzymatic activity even in the absence of upstream phosphorylation by RAF. We also found that signal-dependent activation of disease variants is independent of KSR, a critical signaling adaptor and a recent target of potent allosteric inhibitors (Dhawan *et al.*, 2016). Our results suggest that these inhibitors may be ineffective for individuals with activating mutations in MEK.

Measurements of ERK activation offer a striking example of a context-dependent response to mutations in a ubiquitously expressed pathway component. Depending on their location in the embryo, cells respond to gain-of-function MEK variants with either up-regulating or down-regulating their ERK activation levels. We proposed that this divergent response reflects a feedback loop whereby mutation-imparted constitutive activation of the pathway triggers expression of negative pathway regulators, making it less sensitive to activation by endogenous patterning cues. We provided clear support for this mechanism by identifying the dual specificity ERK phosphatase Mkp3 as a critical component of the hypothesized feedback and showing that RNAi knockdown of *Mkp3* eliminates the divergent response to expression of activating MEK variants. *Mkp3* was also found to be up-regulated in cardiomyocytes from an individual with a developmental abnormality with a germline mutation in RAF, suggesting that this effect is not limited to *Drosophila* (Jaffre *et al.*, 2019). Importantly, we have previously detected CIC binding to the *Mkp3* locus (Keenan *et al.*, 2020). Furthermore, while this study was in review, the mammalian homologue to Mkp3, DUSP6, was demonstrated to be transcriptionally regulated by CIC promoter binding (Ren *et al.*, 2020). Thus, this regulatory loop through Mkp3 is highly conserved. Studies in systems amenable to quantitative imaging, such as the terminal system, offer an opportunity to explore these effects in the most controlled and comprehensive way. We have done this for MEK, but the presented approach can be readily extended to the rest of the RAS pathway (Rauen, 2013; Maher *et al.*, 2018a; Tajan *et al.*, 2018; Taylor *et al.*, 2019). In particular, all of our approaches are directly useful for quantitative investigation of newly discovered human mutations affecting ERK, the only known enzymatic substrate of MEK and an emerging drug target in cancer (Futran *et al.*, 2013; Taylor *et al.*, 2019; Motta *et al.*, 2020; Smorodinsky-Atias *et al.*, 2020).

METHODS AND MATERIALS

Request a protocol through *Bio-protocol*.

Fly stocks

Fly stocks were maintained under standard conditions and crosses were performed at 25°C unless otherwise specified. OregonR, Histone-GFP, MTD-GAL4, UAS-*MEK*WT, UAS-*MEK*F53S, UAS-*MEK*Y130C, and UAS-*MEK*E203K flies were described in Jindal *et al.* (2017b). S218A/S222A were introduced into UAS-MEK^{F53S} construct to generate UAS-MEK$^{F53S\ SSAA}$ with site-directed mutagenesis using Q5 hot start DNA Polymerase (NEB M0493) with the primers mek_218_228S2A_F: CCAACgCCTTTGTGGGCACCCGTA and mek_218_228S2A_R: CCATCGcGTCGATCAGTTGACCGGAG and verified by sequencing. The UAS-MEK$^{F53S\ SSAA}$ construct was integrated into attP40 site using the ΦC31-based integration system. UAS-*ksr RNAi* (41598) and UAS-*RAF* RNAi (41589) were from the

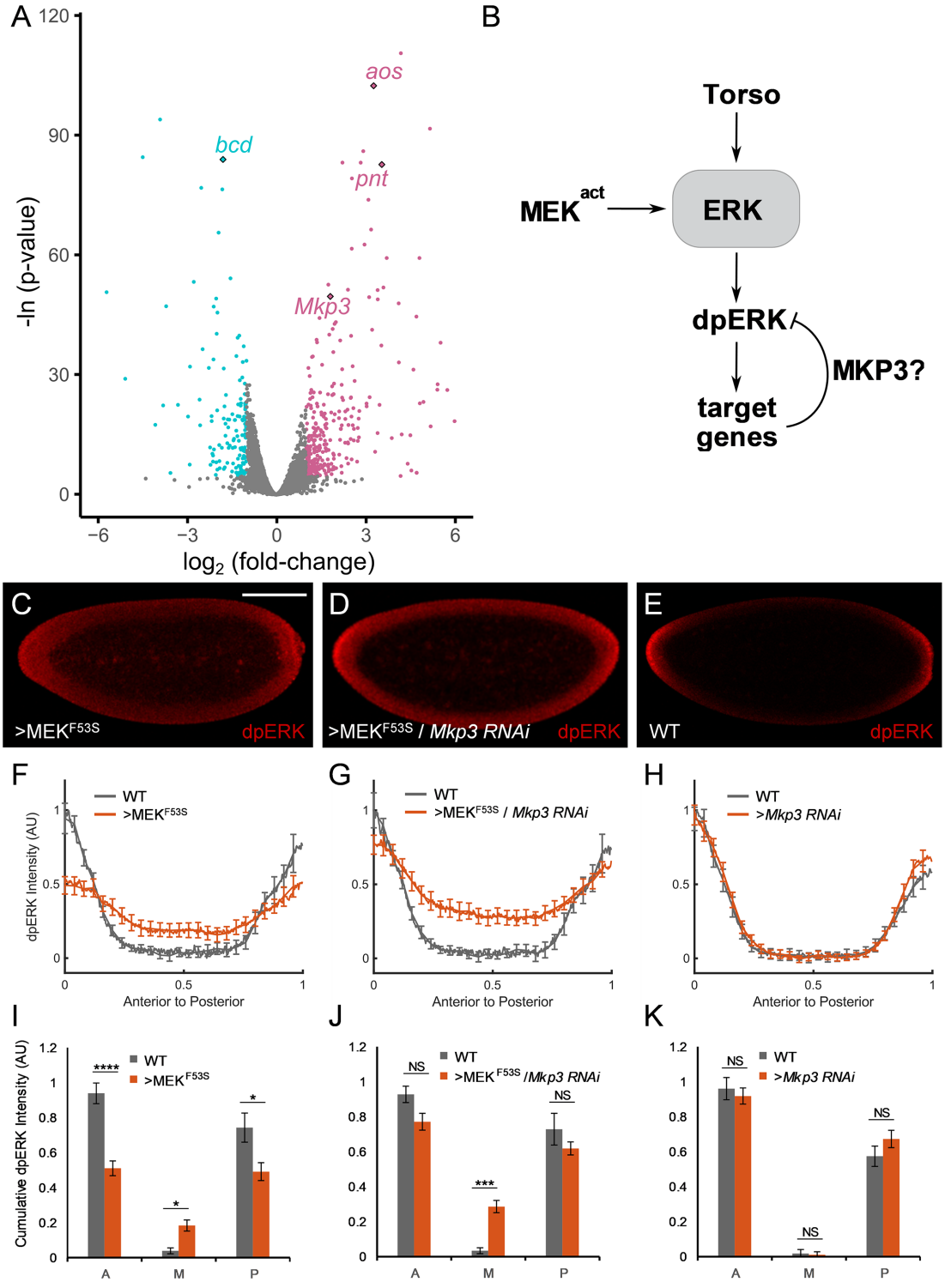

FIGURE 4: Transcriptional feedback attenuating ERK activation by Torso. (A) Volcano plot of maternally deposited mRNA transcript abundance of MTD>MEK^{F53S} vs. MTD>MEK^{WT} (overexpressed WT MEK). All core components of the RAS pathway remain unchanged. Known transcriptional targets of RAS signaling, *pnt* and *aos*, are significantly up-regulated. *Mkp3*, encoding a dual specificity ERK phosphatase is also significantly up-regulated. (B) Model of the negative feedback loop induced by constitutively active MEK. (C–E) Representative images of nuclear cycle 14 embryos stained for active, dually phosphorylated ERK (dpERK) for different genetic backgrounds. Scale bar, 100 µm. (F–H) Pairwise comparison of the spatial dpERK profiles for WT (gray) and mutant (red) embryos. (F) Maternal overexpression of MEK^{F53S} results in ectopic ERK activation in the central positions of the embryo and attenuates RTK-dependent ERK activation at the poles. WT ($n = 6$) and 67;15>MEK^{F53S} ($n = 17$). (G) Disruption of the Mkp3-dependent feedback loop counteracts signal down-regulation at the poles and enhances ectopic ERK activation. WT ($n = 6$) and 67;15>MEK^{F53S} + *Mkp3* RNAi ($n = 23$). (H) Down-regulation of *Mkp3* in embryos without activating MEK has no effect on the pattern of ERK activation. WT ($n = 10$) and 67;15>*Mkp3* RNAi ($n = 19$). (I–K) Comparative analysis of

dpERK levels in the anterior (A), middle (M), and posterior (P). regions of the embryo. The analysis performed corresponds to the same embryo data used to generate the spatial plots in F–H. *P* values were obtained by Student's *t* test (two-sided, homoscedastic): ****$P < 0.0001$, ***$P < 0.001$, *$P < 0.05$, NS: $P > 0.05$. Error bars denote standard error of the mean.

Bloomington *Drosophila* Stock Center. The UAS-*Mkp3 RNAi* line was generated by integrating a previously established RNAi construct HMS04475 (a gift from Norbert Perrimon) onto the third chromosome by ΦC31 integration into attP2 (Sopko *et al.*, 2014). The newly developed fly lines are available on request. Egg lays and embryonic development were conducted at 22°C.

Cuticle phenotyping

Embryos were dechorionated after being aged for more than 24 h as previously reported (Goyal *et al.*, 2017a; Johnson *et al.*, 2017). Dechorionated embryos were shaken in methanol and heptane (1:1) and incubated overnight in a media containing lactic acid and Hoyer's media (1:1) at 65°C. Embryos were imaged on a Nikon Eclipse Ni in darkfield.

Immunostaining and FISH

dpERK antibody staining and *tailless* FISH protocols were performed as described previously (Goyal *et al.*, 2017a). Rabbit anti-dpERK (1:100; Cell Signaling Technology #4370S), sheep anti-GFP (1:1000, Bio-Rad #4745-1051), and sheep anti-digoxigenin (DIG) (1:125; Roche #11333089001) were used as primary antibodies. DAPI (1:10,000; Molecular probes #D1306) was used to stain for nuclei, and Alexa Fluor conjugates (1:500; Invitrogen) were used as secondary antibodies.

Microscopy and image processing

Fluorescent imaging of fixed embryos for immunostaining and FISH experiments were performed on a Nikon A1-RS scanning confocal microscope with a 20× objective, similar to previously reported procedures (Goyal *et al.*, 2017a). For pairwise comparisons of WT and mutant backgrounds, embryos were collected, stained, and imaged together under the same experimental conditions. Our software allows the MEK measurements to be quantified while the experimenter is blinded to the genotype. Broken embryos, embryos with intact vitelline membrane, or embryos undergoing mitosis were excluded from the analysis.

RNA-seq analysis

MTD>*MEK*WT and MTD>*MEK*F53S overexpressing females were mated to sterile males of the *βTub85D*D genotype (Bloomington Stock #2149). One half-hour collections of ~20 embryos were stored at 4°C in RNAlater solution, transferred to TRIzol, and prepped with a TRIzol RNA column from Zymo Research. Directional RNA-seq was conducted in biological triplicates for each genotype by the Princeton Sequencing Core. The raw data and gene expression measurements will be available on NCBI GEO with the accession identifier: GSE162684.

Each RNA-seq library was inspected for quality and subsequently mapped to the fly transcriptome (r6.19) using Salmon (v0.8.2) in quasi-mapping mode with GC content and sequence-specific bias corrections to produce a gene-level read count matrix. Differential expression analysis was performed between the *MEK*WT and the *MEK*F53S replicate per-gene read counts using the edgeR software package's exact test option after removing lowly expressed genes. Specifically, we removed genes with fewer than 1 count per million (corresponding to approximately 37 mapped reads in the smallest library) in at least half of the samples. False discovery rate control was applied to the per-gene *p* values using the Benjamini–Hochberg procedure, and genes with FDR < = 0.01 were determined to be differentially expressed. The limits set on the axes of the volcano plot does limit the display of several extreme examples for visual clarity.

ACKNOWLEDGMENTS

We thank Becky Burdine, Aleena Patel, Shannon Keenan, Bruce Gelb, Ben Neel, Nareg Djabrayan, and Vicki Patterson for many helpful discussions. We thank Gary Laevsky from the Princeton Nikon Imaging Facility for assistance with microscopy as well as the staff of the Sequencing Core Facility of the Lewis-Sigler Institute for help with the RNA-seq experiments. We also thank Kei Yamaya for contributions during the early stages of this work and all members of the Shvartsman Lab for comments and suggestions. This work was supported by National Institutes of Health (NIH) grants R01-GM086537 and R01-HD085870 (awarded to S.Y.S.). Y.G. acknowledges the support of Schmidt Science Fellowship (in partnership with the Rhodes Trust) and the Jane Coffin Childs Memorial Fund for Medical Research for their support. G.A.J. acknowledges support from American Heart Association Grant #18POST34030077 (Award year: 2018). G.A.J. acknowledges past support by the National Science Foundation Graduate Research Fellowship Grant DGE-1148900. National Science Foundation: ABI-1458457 (awarded to M.S.) and DGE-1148900 (awarded to J.W.) and NIH: R01-GM076275 (awarded to M.S.).

REFERENCES

Ashton-Beaucage D, Therrien M (2017). How genetics has helped piece together the MAPK signaling pathway. Methods Mol Biol 1487, 1–21.

Avruch J (2007). MAP kinase pathways: the first twenty years. Biochim Biophys Acta 1773, 1150–1160.

Bentivegna S, Zheng J, Namsaraev E, Carlton VE, Pavlicek A, Moorhead M, Siddiqui F, Wang Z, Lee L, Ireland JS, *et al.* (2008). Rapid identification of somatic mutations in colorectal and breast cancer tissues using mismatch repair detection (MRD). Hum Mutat 29, 441–450.

Brennan DF, Dar AC, Hertz NT, Chao WC, Burlingame AL, Shokat KM, Barford D (2011). A Raf-induced allosteric transition of KSR stimulates phosphorylation of MEK. Nature 472, 366–369.

Bromberg-White JL, Andersen NJ, Duesbery NS (2012). MEK genomics in development and disease. Brief Funct Genomics 11, 300–310.

Casanova J, Struhl G (1989). Localized surface activity of torso, a receptor tyrosine kinase, specifies terminal body pattern in Drosophila. Genes Dev 3, 2025–2038.

Casci T, Vinos J, Freeman M (1999). Sprouty, an intracellular inhibitor of Ras signaling. Cell 96, 655–665.

Caunt CJ, Sale MJ, Smith PD, Cook SJ (2015). MEK1 and MEK2 inhibitors and cancer therapy: the long and winding road. Nat Rev Cancer 15, 577–592.

Chapman PB, Solit DB, Rosen N (2014). Combination of RAF and MEK inhibition for the treatment of BRAF-mutated melanoma: feedback is not encouraged. Cancer Cell 26, 603–604.

Chen X, Mitsutake N, LaPerle K, Akeno N, Zanzonico P, Longo VA, Mitsutake S, Kimura ET, Geiger H, Santos E, *et al.* (2009). Endogenous expression of Hras(G12V) induces developmental defects and neoplasms with copy number imbalances of the oncogene. Proc Natl Acad Sci USA 106, 7979–7984.

Coppey M, Boettiger AN, Berezhkovskii AM, Shvartsman SY (2008). Nuclear trapping shapes the terminal gradient in the Drosophila embryo. Curr Biol 18, 915–919.

Dalton D, Chadwick R, McGinnis W (1989). Expression and embryonic function of empty spiracles: a Drosophila homeo box gene with two patterning functions on the anterior-posterior axis of the embryo. Genes Dev 3, 1940–1956.

Dhawan NS, Scopton AP, Dar AC (2016). Small molecule stabilization of the KSR inactive state antagonizes oncogenic Ras signalling. Nature 537, 112–116.
Duffy JB (2002). GAL4 system in Drosophila: a fly geneticist's Swiss army knife. Genesis 34, 1–15.
Edwards JJ, Gelb BD (2016). Genetics of congenital heart disease. Curr Opin Cardiol 31, 235–241.
Fischmann TO, Smith CK, Mayhood TW, Myers JE, Reichert P, Mannarino A, Carr D, Zhu H, Wong J, Yang RS, *et al.* (2009). Crystal structures of MEK1 binary and ternary complexes with nucleotides and inhibitors. Biochemistry 48, 2661–2674.
Futran AS, Link AJ, Seger R, Shvartsman SY (2013). ERK as a model for systems biology of enzyme kinetics in cells. Curr Biol 23, R972–R979.
Gabay L, Seger R, Shilo BZ (1997). MAP kinase in situ activation atlas during Drosophila embryogenesis. Development 124, 3535–3541.
Gomez AR, Lopez-Varea A, Molnar C, de la Calle-Mustienes E, Ruiz-Gomez M, Gomez-Skarmeta JL, de Celis JF (2005). Conserved cross-interactions in Drosophila and Xenopus between Ras/MAPK signaling and the dual-specificity phosphatase MKP3. Dev Dyn 232, 695–708.
Goyal Y, Jindal GA, Pelliccia JL, Yamaya K, Yeung E, Futran AS, Burdine RD, Schupbach T, Shvartsman SY (2017a). Divergent effects of intrinsically active MEK variants on developmental Ras signaling. Nat Genet 49, 465–469.
Goyal Y, Levario TJ, Mattingly HH, Holmes S, Shvartsman SY, Lu H (2017b). Parallel imaging of Drosophila embryos for quantitative analysis of genetic perturbations of the Ras pathway. Dis Model Mech 10, 923–929.
Goyal Y, Schupbach T, Shvartsman SY (2018). A quantitative model of developmental RTK signaling. Dev Biol 442, 80–86.
Haagenson KK, Wu GS (2010). Mitogen activated protein kinase phosphatases and cancer. Cancer Biol Ther 9, 337–340.
Hanahan D, Weinberg RA (2000). The hallmarks of cancer. Cell 100, 57–70.
Hanahan D, Weinberg RA (2011). Hallmarks of cancer: the next generation. Cell 144, 646–674.
Jaffre F, Miller CL, Schanzer A, Evans T, Roberts AE, Hahn A, Kontaridis MI (2019). Inducible pluripotent stem cell-derived cardiomyocytes reveal aberrant extracellular regulated kinase 5 and mitogen-activated protein kinase kinase 1/2 signaling concomitantly promote hypertrophic cardiomyopathy in RAF1-associated Noonan Syndrome. Circulation 140, 207–224.
Jindal GA, Goyal Y, Burdine RD, Rauen KA, Shvartsman SY (2015). RASopathies: unraveling mechanisms with animal models. Dis Model Mech 8, 769–782.
Jindal GA, Goyal Y, Humphreys JM, Yeung E, Tian K, Patterson VL, He H, Burdine RD, Goldsmith EJ, Shvartsman SY (2017a). How activating mutations affect MEK1 regulation and function. J Biol Chem 292, 18814–18820.
Jindal GA, Goyal Y, Yamaya K, Futran AS, Kountouridis I, Balgobin CA, Schupbach T, Burdine RD, Shvartsman SY (2017b). In vivo severity ranking of Ras pathway mutations associated with developmental disorders. Proc Natl Acad Sci USA 114, 510–515.
Johnson HE, Goyal Y, Pannucci NL, Schupbach T, Shvartsman SY, Toettcher JE (2017). The spatiotemporal limits of developmental Erk signaling. Dev Cell 40, 185–192.
Jurgens G, Wieschaus E, Nusslein-Volhard C, Kluding H (1984). Mutations affecting the pattern of the larval cuticle inDrosophila melanogaster: II. Zygotic loci on the third chromosome. Wilehm Roux Arch Dev Biol 193, 283–295.
Keenan SE, Blythe SA, Marmion RA, Djabrayan NJ, Wieschaus EF, Shvartsman SY (2020). Rapid dynamics of signal-dependent transcriptional repression by capicua. Dev Cell 52, 794–801.e794.
Keyse SM (2008). Dual-specificity MAP kinase phosphatases (MKPs) and cancer. Cancer Metastasis Rev 27, 253–261.
Kim Y, Iagovitina A, Ishihara K, Fitzgerald KM, Deplancke B, Papatsenko D, Shvartsman SY (2013). Context-dependent transcriptional interpretation of mitogen activated protein kinase signaling in the Drosophila embryo. Chaos 23, 025105.
Lavoie H, Sahmi M, Maisonneuve P, Marullo SA, Thevakumaran N, Jin T, Kurinov I, Sicheri F, Therrien M (2018). MEK drives BRAF activation through allosteric control of KSR proteins. Nature 554, 549–553.
Maher GJ, McGowan SJ, Giannoulatou E, Verrill C, Goriely A, Wilkie AO (2016). Visualizing the origins of selfish de novo mutations in individual seminiferous tubules of human testes. Proc Natl Acad Sci USA 113, 2454–2459.
Maher GJ, Ralph HK, Ding Z, Koelling N, Mlcochova H, Giannoulatou E, Dhami P, Paul DS, Stricker SH, Beck S, *et al.* (2018a). Selfish mutations dysregulating RAS-MAPK signaling are pervasive in aged human testes. Genome Res 28, 1779–1790.
Maher GJ, Ralph HK, Ding ZH, Koelling N, Mlcochova H, Giannoulatou E, Dhami P, Paul DS, Stricker SH, Beck S, *et al.* (2018b). Selfish mutations dysregulating RAS-MAPK signaling are pervasive in aged human testes. Genome Research 28, 1779–1790.
Mansour SJ, Candia JM, Matsuura JE, Manning MC, Ahn NG (1996). Interdependent domains controlling the enzymatic activity of mitogen-activated protein kinase kinase 1. Biochemistry 35, 15529–15536.
Motta M, Pannone L, Pantaleoni F, Bocchinfuso G, Radio FC, Cecchetti S, Ciolfi A, Di Rocco M, Elting MW, Brilstra EH, *et al.* (2020). Enhanced MAPK1 function causes a neurodevelopmental disorder within the RASopathy clinical spectrum. Am J Hum Genet 107, 499–513.
Musacchio M, Perrimon N (1996). The Drosophila kekkon genes: novel members of both the leucine-rich repeat and immunoglobulin superfamilies expressed in the CNS. Dev Biol 178, 63–76.
Neben CL, Lo M, Jura N, Klein OD (2019). Feedback regulation of RTK signaling in development. Dev Biol 447, 71–89.
Nikolaev SI, Rimoldi D, Iseli C, Valsesia A, Robyr D, Gehrig C, Harshman K, Guipponi M, Bukach O, Zoete V, *et al.* (2011). Exome sequencing identifies recurrent somatic MAP2K1 and MAP2K2 mutations in melanoma. Nature Genetics 44, 133–139.
Ohren JF, Chen H, Pavlovsky A, Whitehead C, Zhang E, Kuffa P, Yan C, McConnell P, Spessard C, Banotai C, *et al.* (2004). Structures of human MAP kinase kinase 1 (MEK1) and MEK2 describe novel noncompetitive kinase inhibition. Nat Struct Mol Biol 11, 1192–1197.
Ordan M, Pallara C, Maik-Rachline G, Hanoch T, Gervasio FL, Glaser F, Fernandez-Recio J, Seger R (2018). Intrinsically active MEK variants are differentially regulated by proteinases and phosphatases. Sci Rep 8, 11830.
Patel AL, Shvartsman SY (2018). Outstanding questions in developmental ERK signaling. Development 145.
Poulikakos PI, Solit DB (2011). Resistance to MEK inhibitors: should we co-target upstream? Sci Signal 4, pe16.
Rauen KA (1993). Cardiofaciocutaneous syndrome. In: GeneReviews((R)), eds. M.P. Adam, H.H. Ardinger, R.A. Pagon, S.E. Wallace, L.J.H. Bean, K. Stephens, and A. Amemiya, Seattle, WA: University of Washington, Seattle.
Rauen KA (2013). The RASopathies. Annu Rev Genomics Hum Genet 14, 355–369.
Ren Y, Ouyang Z, Hou Z, Yan Y, Zhi Z, Shi M, Du M, Liu H, Wen Y, Shao Y (2020). CIC is a mediator of the ERK1/2-DUSP6 negative feedback loop. iScience 23, 101635.
Roberts PJ, Der CJ (2007). Targeting the Raf-MEK-ERK mitogen-activated protein kinase cascade for the treatment of cancer. Oncogene 26, 3291–3310.
Rodriguez-Viciana P, Tetsu O, Tidyman WE, Estep AL, Conger BA, Cruz MS, McCormick F, Rauen KA (2006). Germline mutations in genes within the MAPK pathway cause cardio-facio-cutaneous syndrome. Science 311, 1287–1290.
Sawamoto K, Okabe M, Tanimura T, Mikoshiba K, Nishida Y, Okano H (1996). The Drosophila secreted protein Argos regulates signal transduction in the Ras/MAPK pathway. Dev Biol 178, 13–22.
Seternes OM, Kidger AM, Keyse SM (2019). Dual-specificity MAP kinase phosphatases in health and disease. Biochim Biophys Acta Mol Cell Res 1866, 124–143.
Smits CM, Shvartsman SY (2020). The design and logic of terminal patterning in Drosophila. Curr Top Dev Biol 137, 193–217.
Smorodinsky-Atias K, Soudah N, Engelberg D (2020). Mutations that confer drug-resistance, oncogenicity and intrinsic activity on the ERK MAP kinases-current state of the art. Cells 9.
Sopko R, Foos M, Vinayagam A, Zhai B, Binari R, Hu Y, Randklev S, Perkins LA, Gygi SP, Perrimon N (2014). Combining genetic perturbations and proteomics to examine kinase-phosphatase networks in Drosophila embryos. Dev Cell 31, 114–127.
Strecker TR, Kongsuwan K, Lengyel JA, Merriam JR (1986). The zygotic mutant tailless affects the anterior and posterior ectodermal regions of the Drosophila embryo. Dev Biol 113, 64–76.
Tajan M, Paccoud R, Branka S, Edouard T, Yart A (2018). The RASopathy family: consequences of germline activation of the RAS/MAPK pathway. Endocr Rev 39, 676–700.
Tartaglia M, Gelb BD (2010). Disorders of dysregulated signal traffic through the RAS-MAPK pathway: phenotypic spectrum and molecular mechanisms. Ann N Y Acad Sci 1214, 99–121.

Taylor CAT, Cormier KW, Keenan SE, Earnest S, Stippec S, Wichaidit C, Juang YC, Wang J, Shvartsman SY, Goldsmith EJ, Cobb MH (2019). Functional divergence caused by mutations in an energetic hotspot in ERK2. Proc Natl Acad Sci USA 116, 15514–15523.

Therrien M, Chang HC, Solomon NM, Karim FD, Wassarman DA, Rubin GM (1995). KSR, a novel protein kinase required for RAS signal transduction. Cell 83, 879–888.

Udell CM, Rajakulendran T, Sicheri F, Therrien M (2011). Mechanistic principles of RAF kinase signaling. Cell Mol Life Sci 68, 553–565.

Yeung E, McFann S, Marsh L, Dufresne E, Filippi S, Harrington HA, Shvartsman SY, Wuhr M (2020). Inference of multisite phosphorylation rate constants and their modulation by pathogenic mutations. Curr Biol 30, 877–882.e876.